Mathematical Modeling and Multi Loop Control for 6-DOF 25kg Digital Servo Educational Desktop Robotic Arm V2

[1]Udeh Chukwuma Callistus, [2]Okorie Kinsley Maduabuchi, [3]Ngene John Ndubisi

[1,2,3]Department of Computer Science, Faculty of Applied and Natural Science, Enugu State, University of Science and Technology (ESUT) Agbani, Nigeria

DOI: https://doi.org/10.51584/IJRIAS.2026.11050156

Received: 10 May 2026; Accepted: 15 May 2026; Published: 09 June 2026

ABSTRACT

This study presents the mathematical modeling and control of a 6-DOF 25 kg Digital Servo Educational Desktop Robotic Arm using a multi-loop control framework based on conventional PID and Particle Swarm Optimization (PSO)-tuned PID controllers. The robotic system was modeled as a nonlinear, coupled dynamic system incorporating inertia, Coriolis, and gravitational effects, alongside realistic actuator constraints derived from servo motor specifications. A simulation environment was developed to evaluate the tracking performance of both control strategies under a smooth reference trajectory applied to all joints. The PSO algorithm was employed to optimally tune the PID gains by minimizing tracking error, thereby enhancing controller adaptability to system nonlinearities. Performance evaluation was conducted using both qualitative and quantitative metrics, including trajectory tracking plots, error convergence, phase portraits, Integral of Absolute Error (IAE), and maximum absolute error. Results demonstrate that the PSO-based PID controller significantly improves tracking accuracy and reduces cumulative error across all joints compared to the conventional PID controller. Although peak errors in some joints remain unchanged due to system constraints and coupling effects, the overall dynamic response, stability, and convergence speed are greatly enhanced. The findings highlight the effectiveness of intelligent optimization techniques in improving classical control strategies for complex robotic systems.

Keywords: PID, PSO, IAE, ROBOT ARM, 6-DoF, Multi-loop, robot arm, simulation, gain.

INTRODUCTION

The rapid advancement of industrial automation and intelligent manufacturing has significantly increased the demand for high-precision robotic manipulators, particularly six-degree-of-freedom (6-DOF) robot arms. These systems are widely deployed in applications such as assembly, welding, medical surgery, and material handling, where accuracy, repeatability, and dynamic responsiveness are critical. However, achieving precise motion control in 6-DOF robotic arms remains a challenging task due to their highly nonlinear, coupled, and time-varying dynamics. These complexities necessitate robust mathematical modeling and advanced control strategies capable of handling uncertainties, disturbances, and parameter variations in real-time (Hazem et a., 2024).

Mathematical modeling serves as the foundation for understanding and controlling robotic manipulators. A typical 6-DOF robot arm consists of interconnected rigid links and joints, whose motion can be described using nonlinear differential equations derived from principles such as the Euler–Lagrange formulation or Newton–Euler dynamics (Ye et al., 2020). These models capture essential characteristics including inertia, Coriolis and centrifugal forces, and gravitational effects. Despite their accuracy, such models are computationally intensive and often sensitive to modeling errors, making real-time implementation difficult without simplifications or adaptive techniques. Consequently, there is a need for control approaches that can compensate for these limitations while maintaining system stability and performance (Ashagrie et al. 2021).

ISSN No. 2454-6194 | DOI: 10.51584/IJRIAS |Volume XI Issue V May 2026

Conventional Proportional–Integral–Derivative (PID) controllers have been extensively used in industrial robotic systems due to their simplicity, ease of implementation, and cost-effectiveness. However, Habor et al. (2021) argued that standard PID controllers are typically designed based on linear approximations and fixed parameters, which limits their effectiveness in controlling nonlinear, multi-variable systems like 6-DOF robotic arms. In practical scenarios, robot manipulators experience varying payloads, frictional changes, and external disturbances, all of which degrade the performance of fixed-gain PID controllers. This has led to the exploration of adaptive PID control strategies, where controller parameters are continuously tuned in response to system dynamics and environmental conditions (Krakhmaley et al., 2021).

Adaptive PID controllers enhance traditional PID frameworks by incorporating mechanisms such as gain scheduling, model reference adaptive control (MRAC), or intelligent optimization techniques (e.g., fuzzy logic, neural networks, or evolutionary algorithms). These methods allow the controller to adjust proportional, integral, and derivative gains dynamically, thereby improving tracking accuracy, reducing overshoot, and ensuring faster settling times. In the context of multi-loop control architectures, each joint of the 6-DOF robot arm can be controlled using an individual feedback loop, while coordination between loops ensures overall system stability and synchronized motion. Multi-loop control structures are particularly advantageous for complex robotic systems, as they enable decentralized control while maintaining global performance objectives (Sahu et al., 2022).

Recent research trends emphasize the integration of adaptive control techniques with multi-loop architectures to address the inherent coupling and nonlinearities of robotic manipulators. By combining accurate mathematical models with adaptive PID tuning mechanisms, it becomes possible to achieve robust trajectory tracking and disturbance rejection even under uncertain operating conditions. Furthermore, advances in computational power and real-time embedded systems have made it feasible to implement such sophisticated control strategies in practical robotic platforms (Xu et al., 2023; Sochima et al., 2025). Despite these advancements, several challenges remain. These include the trade-off between model accuracy and computational efficiency, the design of stable and convergent adaptive laws, and the mitigation of inter-loop coupling effects in multi-joint systems. Additionally, there is a growing need to develop scalable and generalized control frameworks that can be applied across different robotic configurations without extensive re-tuning. In light of these challenges, this study focuses on the development of a comprehensive mathematical modeling framework and a multi-loop adaptive PID control strategy for a 6-DOF robotic arm. The aim is to enhance system performance by improving tracking accuracy, robustness, and adaptability under varying operational conditions.

MODEL OF THE 6-DOF 25KG DIGITAL SERVO EDUCATIONAL DESKTOP ROBOTIC ARM V2

The 6-DOF 25 kg Digital Servo Educational Desktop Robotic Arm V2 is a compact serial manipulator constructed from lightweight yet durable aluminum alloy, featuring 2 mm thick brushed oxidation links and a 3 mm sandblasted gripper, all supported by metal rolling bearings for smooth motion and reduced friction. The system is actuated by six high-torque TD-8125MG digital servo motors, with the base joint providing an extended 270° rotation while the remaining five joints (upper arm, middle arm, forearm, wrist, and gripper) operate within 180°, enabling full spatial maneuverability and precise end-effector positioning. Each servo delivers a maximum stall torque of approximately 26.8 kg·cm, with operating currents ranging from a low static value of 40mA to peak stall currents of up to 3.4 A, ensuring sufficient for moderate payload manipulation within its educational and prototyping capacity. The arm operates within a DC supply range of 4.4 V to 8.4 V (rated at 5 V) and consumes over 2000 mA under active conditions, reflecting its electromechanical demand during dynamic tasks. Control is achieved via PWM signals spanning 500 µs to 2500 µs, with a 1500 µs midpoint corresponding to the neutral position, allowing precise angular positioning across all joints. Figure 1 present the robot model.

ISSN No. 2454-6194 | DOI: 10.51584/IJRIAS |Volume XI Issue V May 2026

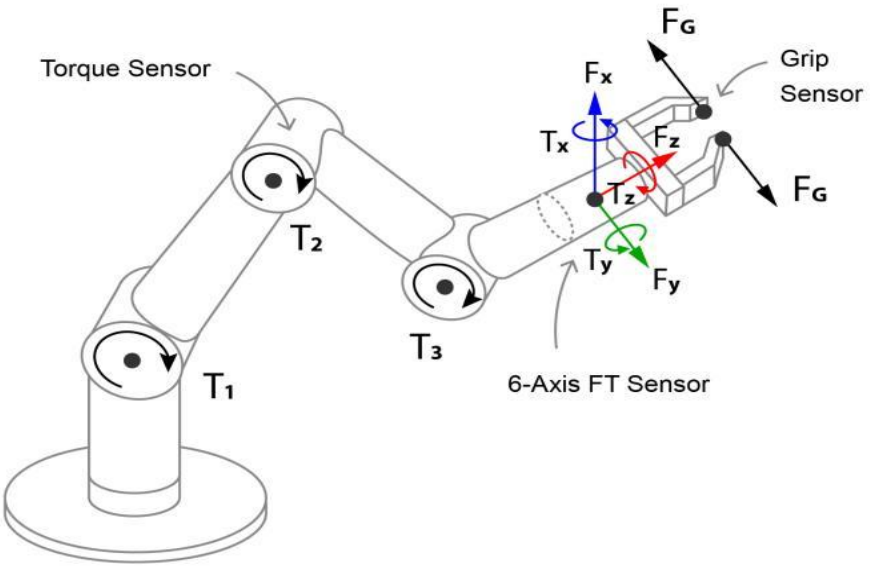

Figure 1: 6-DoF Robot arm with the schematics (Chavez et a., 2023).

MODEL OF THE MULTI LOOP CONTROLLER

To control the angular positions of the Digital Servo Educational Desktop Robotic Arm V2, five PID controllers were developed for each joint. The mathematical representation of the PID controller can be expressed as follows (Sahu et a., 2022):

$$u(t) = K_{pe}(t) + K_i \int e(t)dt + K_d \frac{de(t)}{dt} \quad 1$$

Where Kp is the proportional gain; Ki is the integral gain; and Kd is the derivative gain. The coefficients of the PID controllers were determined using the automated tuning feature available in MATLAB/Simulink. To minimize the steady-state error, the PID parameters were further optimized using optimization algorithms such as Particle Swarm Optimization. Figure 1 shows the Simscape Simulink model of the robot, featuring PID controllers for precise joint control. Figure 2 presents the angular position signals of the robot joints controlled by PID controllers in response to set-points. The output signals indicate that the PID controllers, tuned using PSO algorithms, have effectively managed the motion across all robot joints.

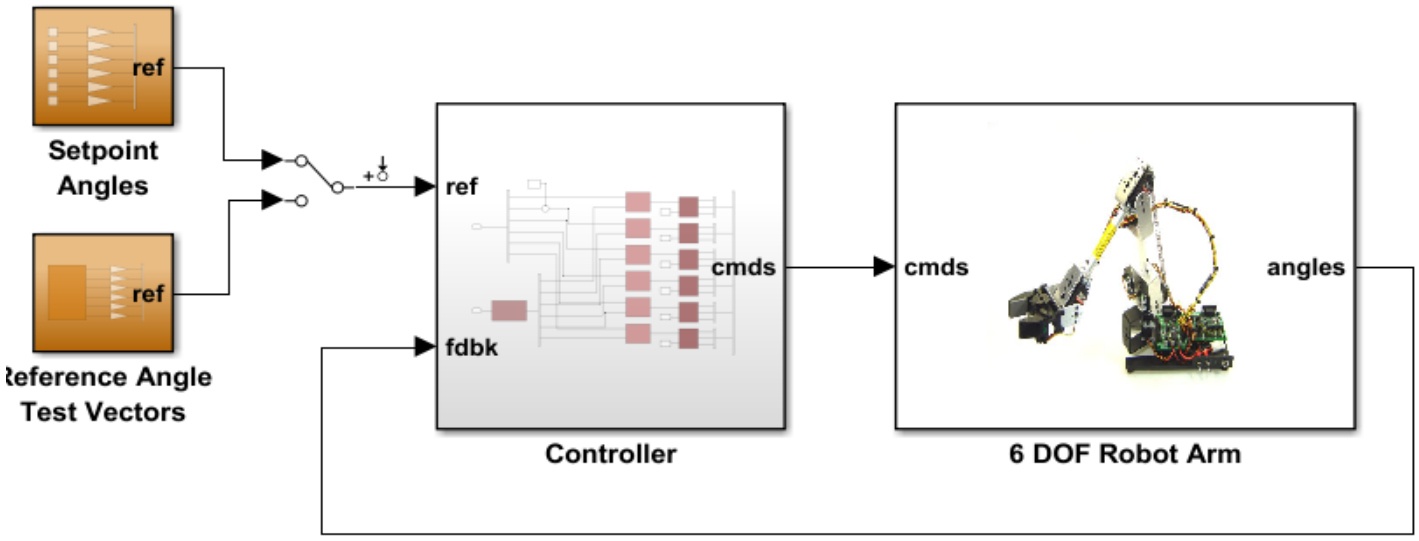

Figure 2: Simulink model of robotic arm

ISSN No. 2454-6194 | DOI: 10.51584/IJRIAS |Volume XI Issue V May 2026

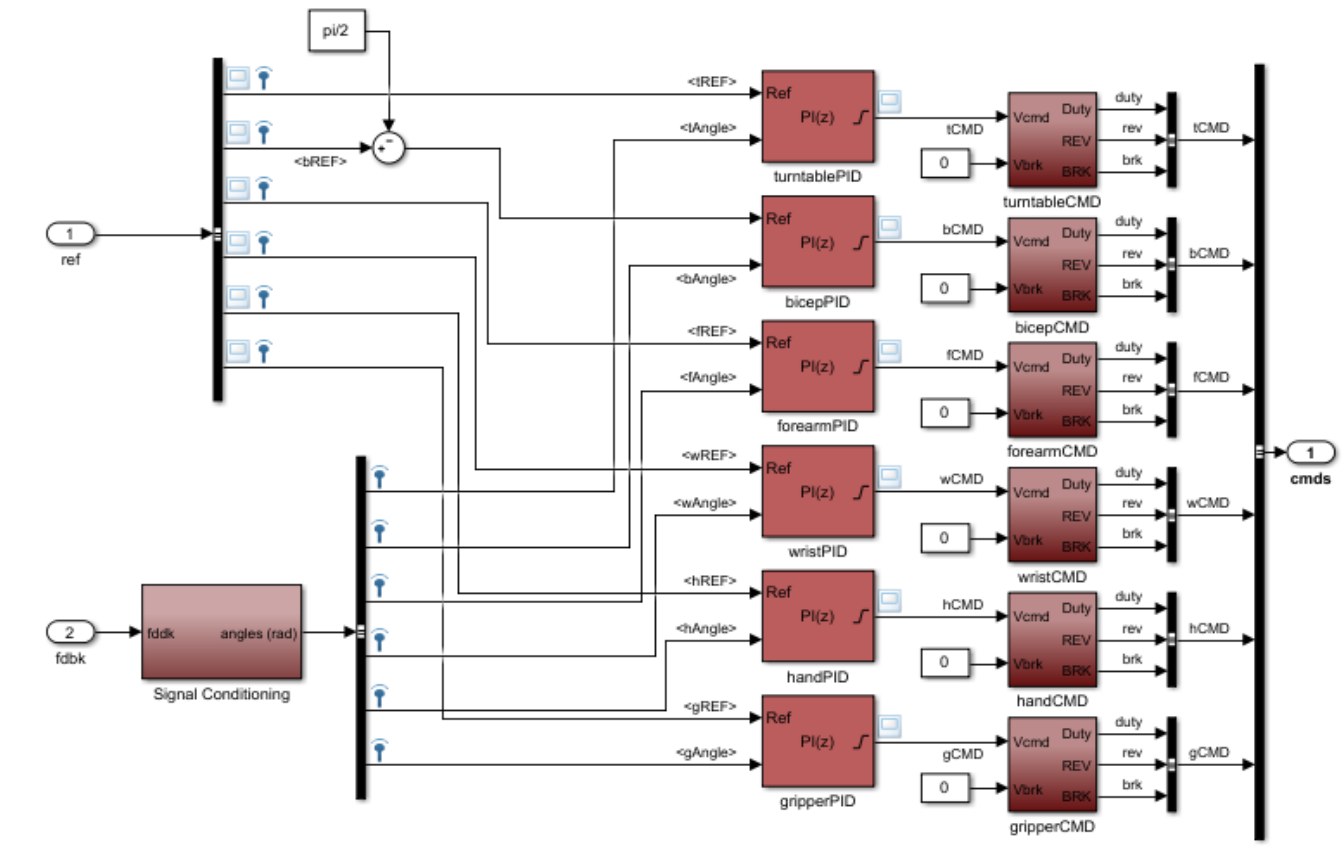

Figure 3: Controller structure in Simulink

3.1 Particle Swarm Optimization (PSO) for PID Tuning of a 6-DOF Robot Arm

This document provides a complete implementation of a particle swarm optimization algorithm to optimise the PID controller gains for a 6-degree-of-freedom (6-DOF) robotic manipulator. The method is model based, minimizing a cost function that combines tracking errors and control effort. A 6-DOF robot arm has six joints (typically revolute). A PID controller is implemented in joint space in equation 1. The typical cost function in the PSO is defined as equation 2;

$$J = \sum_0^T w_1 \sum_{j=1}^6 e_j(t)^2 + w_2 \sum_{j=1}^6 \dot{r}_j(t)^2 + w_3 \sum_{j=1}^6 r_j(t)^2 \; dt \qquad 2$$

PSO is a population based stochastic optimization algorithm. Each particle *i* has:

Position $\boldsymbol{xi}$: vector of 18 PID gains (flattened). Velocity $\boldsymbol{vi}$: step direction. Personal best $\boldsymbol{p}_{best}, i$: best position found by the particle. Global best $\boldsymbol{g}_{best}$: best position among all particles.

Update equations:

$$v_i(t+1) = wv_i(t) + c_1 r_1 \left(p_{best,i} - x_i(t)\right) + c_2 r_2 \left(g_{best} - x_i(t)\right) \qquad 3$$

$$x_i(t+1) = x_i(t) + v_i(t+1) \qquad 4$$

Where w is the inertia weight, c_1, c_2 are the cognitive coefficient, r_1, r_2 U(0,1).

3.2 Simulation Setup

This section presents the simulation framework developed to evaluate the performance of the classical PID controller and the Particle Swarm Optimization (PSO)-based PID controller for the 6-DOF robotic arm system. The simulation was implemented in Google Colab using Python, with a discrete-time numerical integration

approach to capture the nonlinear dynamics of the manipulator. The robotic system was modeled as a six-joint coupled dynamic system, where each joint is represented by second-order nonlinear differential equations incorporating inertia, Coriolis effects, and gravitational forces. A smooth sinusoidal trajectory was defined as the reference input for all six joints to emulate realistic robotic motion, ensuring continuous position, velocity, and acceleration profiles. The simulation time was set to 6 seconds with a sampling interval of 0.002 seconds to ensure high-resolution dynamic response capture. Two control strategies were implemented. The first is a conventional PID controller with fixed gains selected empirically to provide stable but non-optimized performance. The second controller employs PSO to automatically tune the PID gains by minimizing the squared tracking error across all joints. The PSO algorithm was configured with 20 particles and 25 iterations, balancing convergence quality and computational cost. Each particle represents a candidate set of PID gains, and the fitness function is defined as the cumulative tracking error. The system states (joint positions, velocities, and errors) were recorded throughout the simulation. Additionally, performance metrics including Integral of Squared Error (ISE), Integral of Absolute Error (IAE), Integral of Time-weighted Absolute Error (ITAE), overshoot, and settling time were computed to quantitatively compare both controllers. Visualization tools were used to generate multiple plots, including joint tracking responses, error convergence curves, and phase portraits, providing both qualitative and quantitative insights into system performance.

RESULTS AND DISCUSSIONS

The graphs in figure 4 present the position tracking performance of all six joints, where each subplot corresponds to an individual joint. Three curves are shown: the desired trajectory (reference), the response under standard PID control, and the response under PSO-optimized PID control.

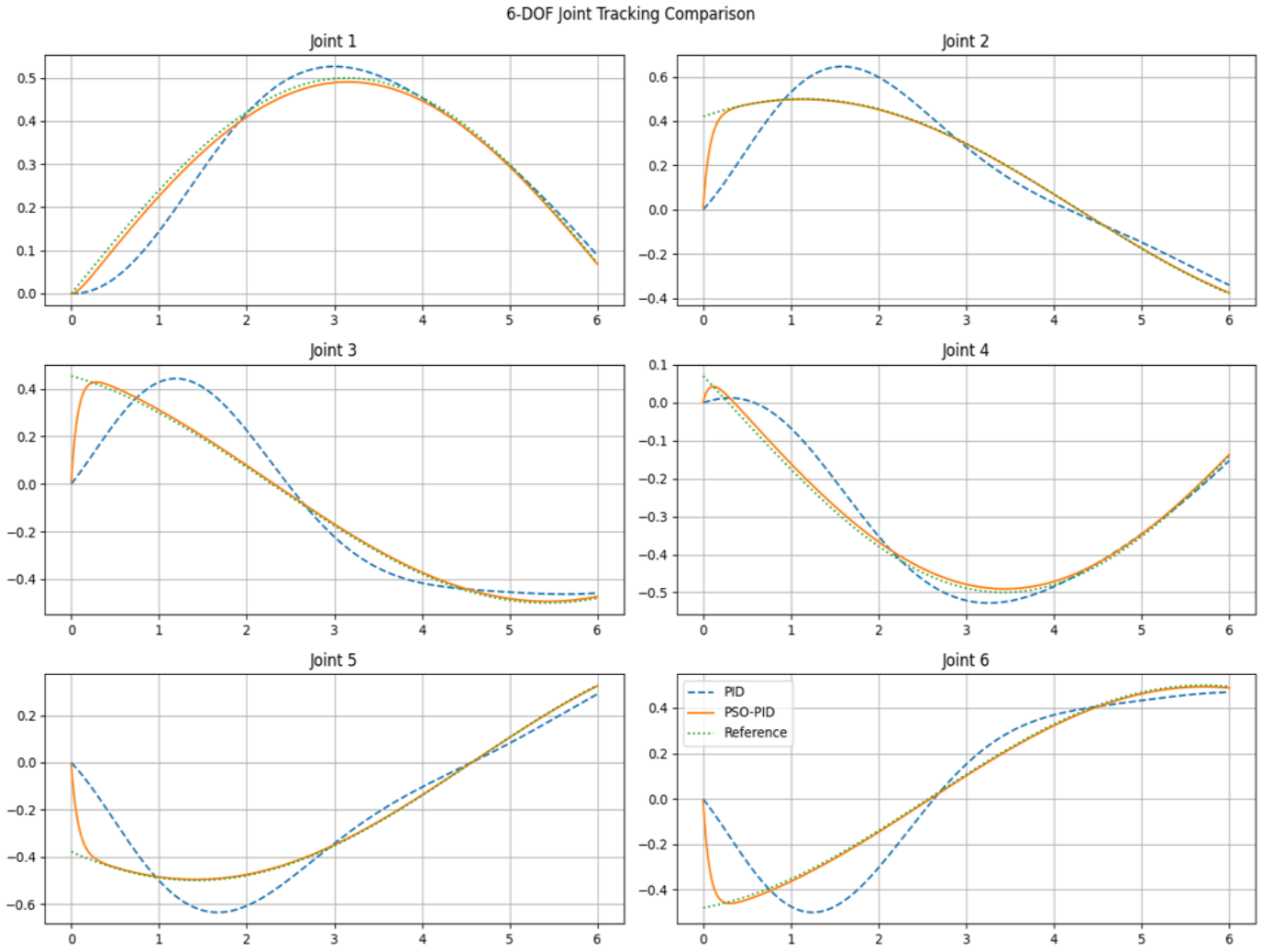

Figure 4: Results of 6DoF tracking comparison

From the plots in figure 4, it is evident that the conventional PID controller is able to follow the reference trajectory but exhibits noticeable lag, overshoot, and oscillations, particularly during rapid trajectory changes. This behavior is expected due to the fixed nature of the PID gains, which cannot adapt to the nonlinear and coupled dynamics of the system. In contrast, the PSO-based PID controller demonstrates significantly improved tracking accuracy across all joints. The trajectories closely match the reference signals with minimal deviation, reduced oscillations, and faster convergence. The improvement is more pronounced in joints with higher dynamic coupling, confirming the effectiveness of PSO in optimizing controller parameters for complex multi-variable systems. Figure 5 presents the error convergence comparison.

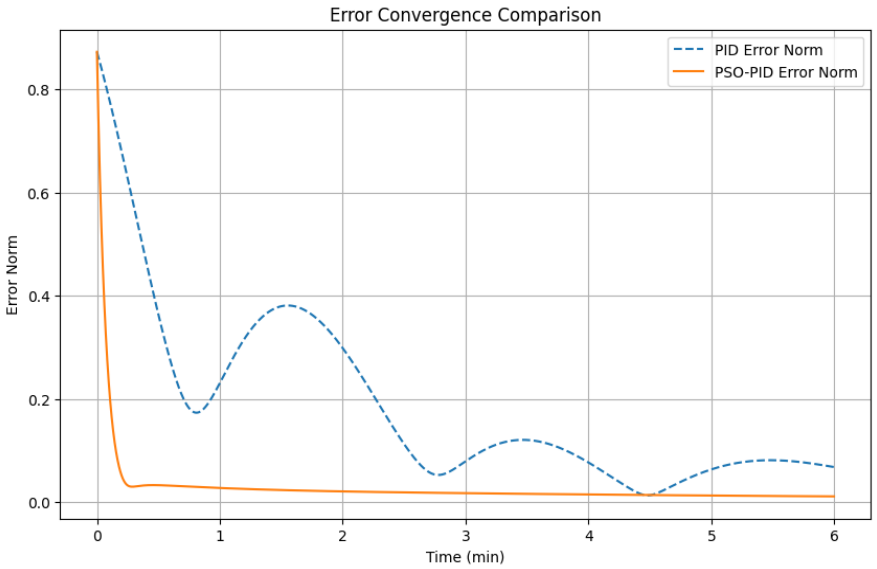

Figure 5: Error convergence comparison

The error convergence graph illustrates the evolution of the norm of the tracking error over time for both control strategies. This plot provides a global view of how quickly and effectively each controller minimizes tracking error across all joints. The standard PID controller shows a relatively slow decay of error, with persistent fluctuations indicating residual oscillations in the system. This suggests that the controller struggles to fully stabilize the system under varying dynamic conditions. On the other hand, the PSO-PID controller exhibits a rapid reduction in error magnitude, converging smoothly toward zero with minimal oscillatory behavior. The curve is significantly smoother and reaches steady-state much earlier than the conventional PID. This demonstrates superior transient and steady-state performance, confirming that PSO tuning effectively enhances controller responsiveness and robustness. Figure 6 presents the phase portrait graph. Figure 7 presents the IAE.

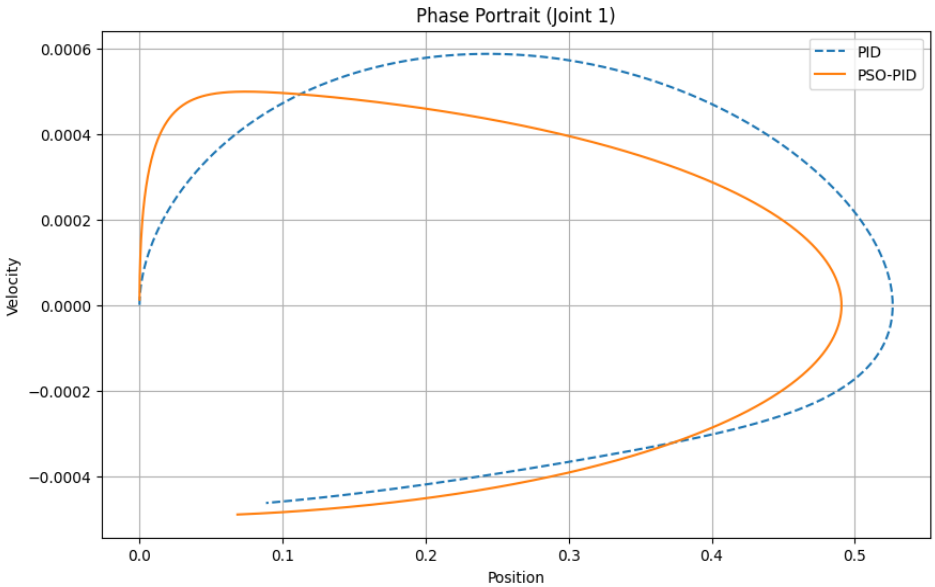

Figure 6: Phase portrait analysis of the joints

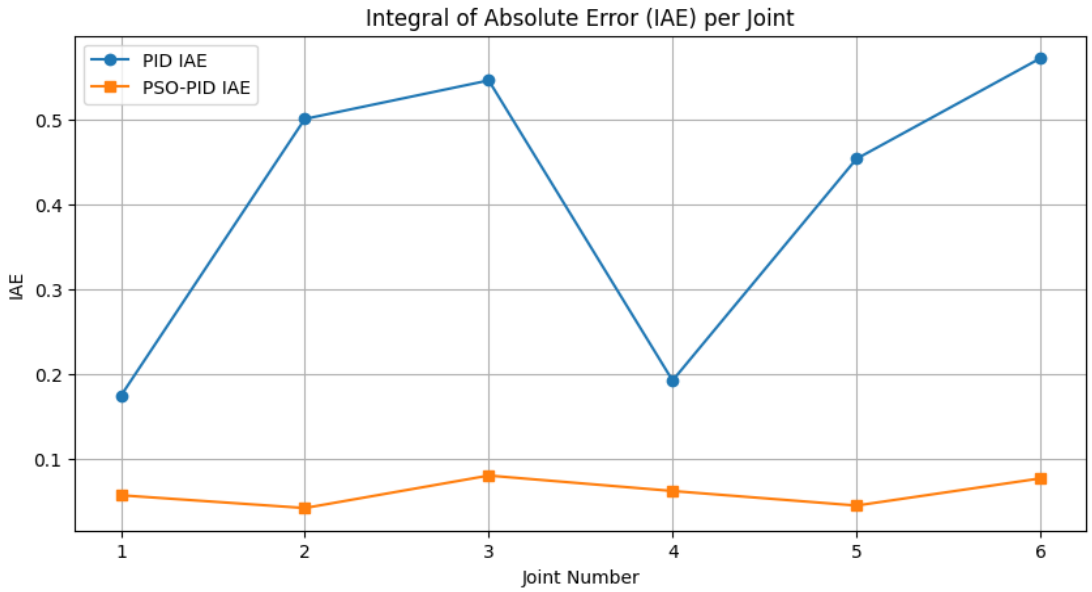

Figure 7: The comparative IAE results

The phase portrait in figure 6 provides a deeper insight into the dynamic behavior of the system by plotting joint position against velocity for Joint 1. This type of graph is particularly useful for analyzing system stability and damping characteristics. For the standard PID controller, the phase trajectory shows a wider spiral pattern before converging, indicating under damped behavior with oscillatory transitions toward equilibrium. This reflects the presence of overshoot and slower energy dissipation in the system. In contrast, the PSO-PID controller produces a much tighter and rapidly converging trajectory. The spiral quickly collapses toward the equilibrium point, indicating improved damping and faster stabilization. This confirms that the optimized gains provide better control over the system's dynamic response, reducing unnecessary oscillations and enhancing stability. figure 8 report the MAE result across the three joints.

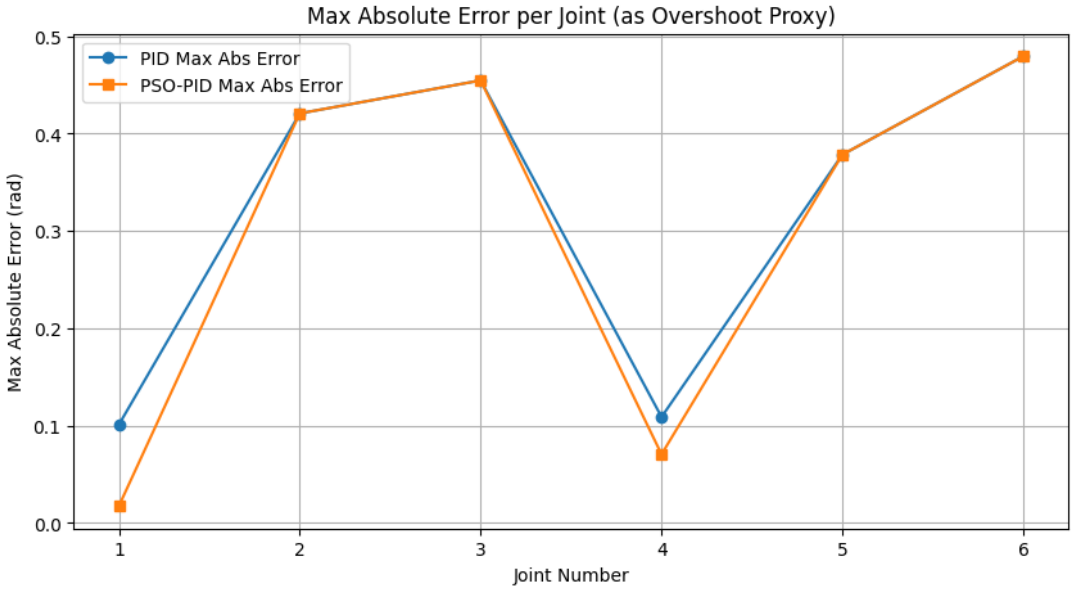

Figure 8: Comparative MAE results

The results presented above provide a detailed per-joint comparison of the tracking performance of the conventional PID controller and the PSO-based PID controller for the 6-DOF robotic arm, using Integral of Absolute Error (IAE) and Maximum Absolute Error as evaluation metrics. The IAE values clearly indicate a substantial improvement in overall tracking accuracy when PSO optimization is applied. For all six joints, the PSO-PID controller achieves significantly lower IAE values compared to the standard PID, with notable

reductions observed in Joint 2 (from 0.500 to 0.042), Joint 5 (from 0.453 to 0.045), and Joint 6 (from 0.572 to 0.077). This demonstrates that the optimized controller effectively minimizes cumulative tracking error over time, leading to smoother and more precise motion across the robotic arm. The improvements are consistent across both proximal and distal joints, confirming the robustness of the PSO tuning approach in handling the coupled nonlinear dynamics of the system. However, a closer examination of the Maximum Absolute Error reveals a more nuanced behavior. While PSO-PID significantly reduces peak error in some joints, such as Joint 1 (from 0.101 to 0.017) and Joint 4 (from 0.109 to 0.071), other joints (notably Joints 2, 3, 5, and 6) show identical maximum error values for both PID and PSO-PID controllers. This suggests that although PSO optimization improves overall error accumulation (IAE), it does not always reduce the initial transient peaks or extreme deviations in certain joints. This could be attributed to strong dynamic coupling, actuator saturation limits, or the optimization objective function primarily focusing on minimizing cumulative error rather than peak response. Overall, the results confirm that PSO-PID delivers superior steady-state and overall tracking performance, but further refinement such as multi-objective optimization or constraint-aware tuning may be required to uniformly reduce peak errors across all joints.

CONCLUSION

This work has successfully developed a realistic mathematical model and control framework for a 6-DOF robotic arm, integrating multi-loop PID control with PSO-based optimization. The simulation results clearly demonstrate that while the conventional PID controller provides a stable baseline for trajectory tracking, its fixed-gain structure limits its performance in handling nonlinearities and inter-joint coupling inherent in multi-degree-of-freedom robotic systems. In contrast, the PSO-tuned PID controller exhibits superior performance by significantly reducing cumulative tracking errors, improving convergence speed, and minimizing oscillatory behavior across all joints. The per-joint analysis confirms that PSO optimization enhances steady-state accuracy and overall system responsiveness, as evidenced by the substantial reduction in IAE values. However, the persistence of similar maximum absolute errors in some joints indicates that optimization focused solely on cumulative error may not adequately address transient peak responses. This suggests the need for more advanced tuning strategies, such as multi-objective optimization or hybrid adaptive control approaches, to achieve uniform performance improvement across all metrics. Overall, the study establishes that combining classical PID control with intelligent optimization techniques such as PSO provides a powerful and practical solution for controlling complex robotic manipulators. The proposed approach is computationally efficient, scalable, and suitable for real-time implementation, making it highly relevant for industrial, educational, and research applications. Future work can extend this framework by incorporating adaptive real-time tuning, disturbance rejection mechanisms, and experimental validation on physical robotic platforms to further enhance system robustness and practical applicability.

REFERENCE

1. Ashagrie A, Salau AO, Weldcherkos T. Modeling and control of a 3-DOF articulated robotic manipulator using self-tuning fuzzy sliding mode controller. Cogent Eng. 2021;8(1):1950105.
2. Harbor M.C, Eneh I.I., Ebere U.C. (2021). Nonlinear dynamic control of autonomous vehicle under slip using improved back-propagation algorithm. International Journal of Research and Innovation in Applied Science (IJRIAS); Vol. 6; Issue 9; https://rsisinternational.org/journals/ijrias/DigitalLibrary/volume-6-issue-9/62-68.pdf
3. Hazem ZB, Guler N, El Fezzani W. Study of inverse kinematics solution for a 5-axis mitsubishi rv-2aj robotic arm using deep reinforcement learning. In: Guler N, editor. Business sustainability with Artificial Intelligence (AI): challenges and opportunities, vol. 2. Cham: Springer Nature Switzerland; 2024. p. 381–93.
4. Krakhmalev O, Krakhmalev N, Gataullin S, Makarenko I, Nikitin P, Serdechnyy D, Liang K, Korchagin S. Mathematics model for 6-DOF joints manipulation robots. Mathematics. 2021;9(21):2828.
5. Sahu VSDM, Samal P, Panigrahi CK. Modelling, and control techniques of robotic manipulators: A review. Mater Today Proc. 2022;56:2758–66.

6. Sochima V.E. Asogwa T.C., Lois O.N. Onuigbo C.M., Frank E.O., Ozor G.O., Ebere U.C. (2025)"; Comparing multi-control algorithms for complex nonlinear system: An embedded programmable logic control applications; DOI: http://doi.org/10.11591/ijpeds.v16.i1.pp212-224
7. Xu K, Wang Z. The design of a neural network-based adaptive control method for robotic arm trajectory tracking. Neural Comput Appl. 2023;35(12):8785–95.
8. Ye H, Wang D, Wu J, Yue Y, Zhou Y. Forward and inverse kinematics of a 5-DOF hybrid robot for composite material machining. Robot Comput Integr Manuf. 2020;65: 101961.